

Low- and high-field transport properties of pseudomorphic $\text{In}_x\text{Ga}_{1-x}\text{As}/\text{In}_{0.52}\text{Al}_{0.48}\text{As}$ ($0.53 < x < 0.65$) modulation-doped heterostructures

W.-P. Hong,^{a)} G. I. Ng, P. K. Bhattacharya, D. Pavlidis, and S. Willing
Center for High-Frequency Microelectronics and Solid State Electronics Laboratory, Department of Electrical Engineering and Computer Science, The University of Michigan, Ann Arbor, Michigan 48109-2122

B. Das
School of Electrical Engineering, Purdue University, West Lafayette, Indiana 47907

(Received 15 February 1988; accepted for publication 4 May 1988)

We have grown pseudomorphic $\text{In}_x\text{Ga}_{1-x}\text{As}/\text{In}_{0.52}\text{Al}_{0.48}\text{As}$ modulation-doped heterostructures by molecular-beam epitaxy under carefully controlled growth conditions. Mobilities as high as 13 900, 74 000, and 134 000 $\text{cm}^2/\text{V s}$ are measured at 300, 77, and 4.2 K in a heterostructure with $x = 0.65$. Shubnikov-de Haas measurements indicate that the change in the effective mass with increasing In is not significant and is not responsible for the enhancement in mobilities. We believe that the improvement results from reduced alloy scattering, reduced intersubband scattering, and reduced impurity scattering, all of which result from a higher conduction-band offset and increased carrier confinement in the two-dimensional electron gas. The high-field electron velocities have been measured in these samples using pulsed current-voltage and pulsed Hall measurements. A monotonic increase in velocities is observed both at 300 and 77 K with an increase of In content in the channel. Velocities of 1.55×10^7 and 1.87×10^7 cm/s are measured at 300 and 77 K, respectively, in a $\text{In}_{0.65}\text{Ga}_{0.35}\text{As}/\text{In}_{0.52}\text{Al}_{0.48}\text{As}$ modulation-doped heterostructure.

I. INTRODUCTION

Pseudomorphic $\text{In}_x\text{Ga}_{1-x}\text{As}/\text{In}_{0.52}\text{Al}_{0.48}\text{As}$ ($x > 0.53$) modulation-doped (MD) heterostructures have emerged as excellent candidates for the design and fabrication of high-frequency and high-speed field-effect transistors.¹⁻⁵ Improvements in the mobilities¹⁻³ and device performance^{4,5} have been observed in modulation-doped field-effect transistors (MODFETs) made with this pseudomorphic system, compared with those in lattice-matched $\text{In}_{0.53}\text{Ga}_{0.47}\text{As}/\text{In}_{0.52}\text{Al}_{0.48}\text{As}$ MODFETs. Some of the improvements in the device performance result from a larger conduction-band discontinuity, leading to a more efficient modulation doping and better confinement. However, it is not clear how the transport properties in the pseudomorphic channels behave at high electric fields and there is no experimental evidence of the degree of reduction in the effective masses.

In order to understand some of these properties of the pseudomorphic heterostructures, we have made a systematic study of their low- and high-field transport properties and have estimated the electron effective masses from temperature-dependent Shubnikov-de Haas measurements. The $\text{In}_x\text{Ga}_{1-x}\text{As}/\text{In}_{0.52}\text{Al}_{0.48}\text{As}/\text{InP}$ MODFET structures had x varying from 0.53 (lattice matched) to 0.65 and were grown by molecular-beam epitaxy. Hall mobilities measured in these structures are the highest ever achieved for the compositions considered. It is apparent that the major improvement in device performance with increase of strain might result from a systematic increase of the high-field carrier velocities and mobilities in the two-dimensional electron gas (2DEG) channel.

II. EXPERIMENTAL TECHNIQUES

Lattice-matched and pseudomorphic $\text{In}_x\text{Ga}_{1-x}\text{As}/\text{In}_{0.52}\text{Al}_{0.48}\text{As}$ MD heterostructures were grown on semi-insulating InP (Fe) substrates in a RIBER 2300 MBE system. The system preparation is briefly described. The effusion cells without the crucibles were baked at 1400 °C for 10 h. Clean PBN crucibles were next loaded into the cells and were baked at temperatures ranging from 1300 to 1500 °C for 11 h. The growth charges consisting of 7N In, 8N Ga, 7N As, 6N Al, and the dopant species (Si) were loaded into the individual cells and the growth chamber was evacuated to $\sim 10^{-9}$ Torr. Background impurities were further reduced by baking the In source in a pure H_2 atmosphere for 16-24 h at 700 °C before loading into the effusion cell. The source materials were then baked for 6-7 h at 100-200 °C above their normal operating temperatures. Substrate temperature for the growth of the entire structure was 500 °C as set in the temperature controller. The growth rate was $\sim 1.1 \mu\text{m/h}$.

The schematic diagram of the structures and corresponding band diagrams are shown in Fig. 1. The MD heterostructures consist of a 0.4- μm undoped $\text{In}_{0.52}\text{Al}_{0.48}\text{As}$ buffer, a 400-Å undoped $\text{In}_{0.53}\text{Ga}_{0.47}\text{As}$ layer, a 150-Å undoped $\text{In}_x\text{Ga}_{1-x}\text{As}$ channel, a 100-Å undoped $\text{In}_{0.52}\text{Al}_{0.48}\text{As}$ spacer layer, a 200-Å Si-doped ($3 \times 10^{18} \text{ cm}^{-3}$) $\text{In}_{0.53}\text{Al}_{0.48}\text{As}$ layer, a 300-Å undoped $\text{In}_{0.52}\text{Al}_{0.48}\text{As}$ layer, and finally a 200-Å Si-doped ($3 \times 10^{18} \text{ cm}^{-3}$) $\text{In}_{0.53}\text{Ga}_{0.47}\text{As}$ for ohmic contacts. Three types of samples were grown with different In mole fractions in the $\text{In}_x\text{Ga}_{1-x}\text{As}$ channel region: $x = 0.53, 0.60,$ and 0.65 . Growth interruptions for 1 min were used at the interface before the $\text{In}_x\text{Ga}_{1-x}\text{As}$ channel to accomplish higher In mole fractions by changing the Ga fluxes.

The dependence of the electron transport properties on the In mole fraction in the channel was investigated by low-

^{a)} Present address: Bell Communications Research, Red Bank, NJ 07701-7020.

n	InGaAs	3 E18	200A
i	InAlAs		300A
n	InAlAs	3E18	200A
i	InAlAs		100A
i	In(x)Ga(1-x)As		150A
i	InGaAs		400A
i	InAlAs		4000A
i	InAlAs/inGaAs		S.L.
S.f.	InP	(100)	

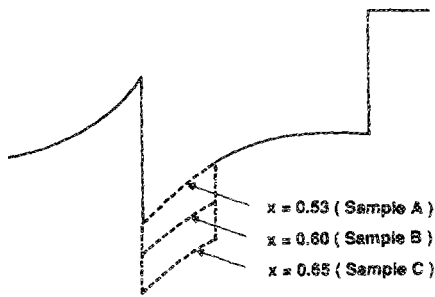


FIG. 1. Schematic of pseudomorphic modulation-doped heterostructures and corresponding band diagrams.

and high-field transport measurements. Cloverleaf and Hall bar geometries were used for low-field Hall measurements by the Van der Pauw technique and Shubnikov-de Haas measurements, respectively. The samples were made from the different structures by photolithography and wet chemical mesa etching with $\text{H}_3\text{PO}_4\text{:H}_2\text{O}_2\text{:H}_2\text{O}$. $\text{Ge}(500 \text{ \AA})/\text{Au}(1200 \text{ \AA})/\text{Ni}(100 \text{ \AA})/\text{Ti}(500 \text{ \AA})/\text{Au}(1000 \text{ \AA})$ contacts were formed by electron-beam evaporation and rapid thermal annealing. Hall mobilities and carrier concentrations were measured in the dark in the temperature range of 4.2–300 K. SdH measurements were made at several temperatures between 1.3 to 4.2 K.

The high-field transport properties were determined from pulsed current-voltage measurements on planar H-shaped devices at 300 K, and pulsed Hall measurements at 300 and 77 K on Hall bars.⁶ The electric field during the current-voltage measurements was determined from the measured potential profile in the bridge region of the device. The H-shaped device geometry ensures that possible domains nucleating near the contacts will not propagate into the bridge region and interfere with the measurement when true current instabilities occur. The voltage pulse width was varied from 0.2 to 1.0 μs . The input and output voltage pulses were recorded on a sampling oscilloscope. The room-temperature electron velocities were computed from the currents measured during the pulsed current-voltage temperatures while the low-temperature (77 K) electron velocities were calculated from the mobility-field characteristics determined by the pulsed Hall measurements.

III. RESULTS AND DISCUSSIONS

A. Low-field transport

Temperature-dependent Hall mobilities measured in the various samples are shown in Fig. 2. At low temperatures, the mobilities increase slowly, indicating the two-dimensional characteristics of carriers in the channel. The sheet electron concentrations decreased from 1.65×10^{12} , 1.79×10^{12} , and $1.82 \times 10^{12} \text{ cm}^{-2}$ at 300 K to 1.50×10^{12} , 1.72×10^{12} , and $1.76 \times 10^{12} \text{ cm}^{-2}$ at 13 K in samples A, B, and C, respectively. Mobility and carrier concentration data at 300 and 77 K for the three samples are summarized in Table I. As can be seen, the increase in the sheet carrier concentration with the addition of excess In is modest. With 65% In in the channel, a carrier density increase of approximately 10% is obtained with the same doping. This is higher than a predicted value of 5% in Ref. 1. The band gap of the $\text{In}_x\text{Ga}_{1-x}\text{As}$ channel material decreases with the increase of In mole fraction, leading to an increase in the conduction-band discontinuity and better confinement. The latter leads to the observed increase in 2DEG carrier concentration.

A noticeable feature in Fig. 2 is the monotonic increase in 2DEG mobility for temperatures $T < 300$ K. The increase in mobility can be attributed to an increase of the momentum relaxation time of carriers from scatterings and/or a decrease of the effective mass of the electrons in the direction parallel to the interface. We have made Shubnikov-de Haas measurements to determine the electron effective masses in the channel of these heterostructures. The masses were derived from the temperature dependence of the SdH oscillation amplitude. Effective masses as well as other electronic properties such as carrier concentration in each subband and energy separation between ground and first excited subbands, computed from the SdH measurement data, are given in Table II. It has been predicted that the electron mass decreases by about 6% with a 12% excess In mole fraction in the channel.¹ However, as can be seen from Table II, the electron mass remains almost constant. This may be due to the fact that strain reduces the crystal symmetry from cubic

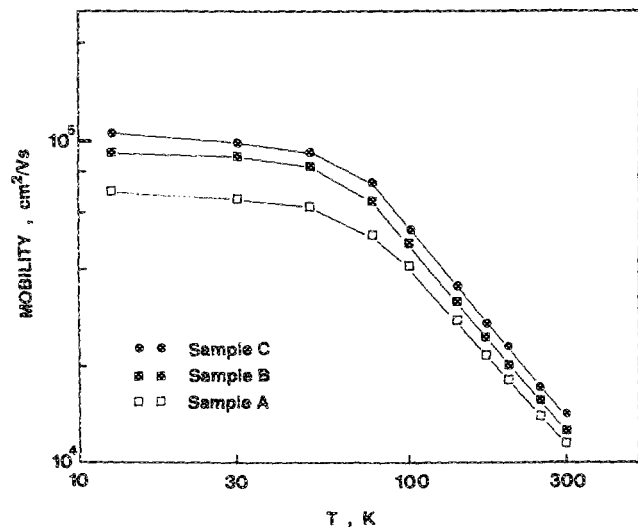


FIG. 2. Temperature-dependent Hall mobilities measured in samples A, B, and C.

TABLE I. Measured Hall data from $\text{In}_x\text{Ga}_{1-x}\text{As}/\text{In}_{0.52}\text{Al}_{0.48}\text{As}$ heterostructure.

Sample	Channel composition	Mobility ($\text{cm}^2/\text{V s}$)		2DEG density (10^{12}cm^{-2})	
		300 K	77 K	300 K	77 K
A	0.53	11 500	50 100	1.65	1.60
B	0.60	12 300	65 200	1.79	1.74
C	0.65	13 900	74 000	1.82	1.79

to tetragonal. Detailed theoretical and experimental studies are required to understand this behavior. It should be noted that the masses derived from SdH measurements are not quite as accurate as those obtained from cyclotron resonance measurements. It is, however, not unreasonable to conclude that the improvement in mobility is from reductions in carrier scattering.

Several scattering mechanisms need to be considered to explain the enhancement in mobility by adding excess In in the channel. At high temperatures, the mobilities are limited mainly by the combination of alloy scattering and optical phonon scattering, whereas at low temperatures, it is mainly alloy scattering that limits the mobility. In the high-temperature region, the slopes of the temperature dependence of mobility are -1.10 and -1.22 for sample A ($x = 0.53$) and sample C ($x = 0.65$), respectively. It has been shown from theoretical calculations^{7,8} that the mobility limited by alloy scattering in the 2DEG system is constant and independent of the temperature, as long as the sheet carrier density remains unchanged. The slope of the temperature-dependent mobility limited by optical phonon scattering is approximately -2.0 .^{9,10} Therefore, it is conceivable that the combination of optical phonon and alloy scattering can result in a slope of ~ -1.0 in the high-temperature region. The more negative slope in the data of sample C with 65% In in the channel is believed to be due to reduced alloy scattering. This is supported by the large enhancement in the low-temperature mobilities in sample C.

The effect of remote ionized impurity scattering is dependent on the carrier density in the channel. The addition of excess In in the channel results in an increase in the conduction-band discontinuity, causing an improvement in carrier confinement and, therefore, an increase of carrier concentration in the channel. Because of this, remote ionized impurity scattering will be reduced due to increased screening, resulting in a higher mobility.

Another important mobility-limiting mechanism is intersubband scattering. The second subband begins to get occupied at carrier densities greater than $4.5 \times 10^{11} \text{cm}^{-2}$.¹¹ The occupation of electrons in the lowest energy subband has been estimated¹ and it increases from 77% in an $\text{In}_{0.53}\text{Ga}_{0.47}\text{As}$ channel to 85% in an $\text{In}_{0.65}\text{Ga}_{0.35}\text{As}$ channel. The band offsets both at the $\text{In}_x\text{Ga}_{1-x}\text{As}/\text{In}_{0.52}\text{Al}_{0.48}\text{As}$ heterointerface and at the $\text{In}_x\text{Ga}_{1-x}\text{As}/\text{In}_{0.52}\text{Al}_{0.48}\text{As}$ heterointerface increase with increasing x as shown in Fig. 1. The built-in potential well enhances the confinement of electrons and increases the energy separation between subbands. The mobility of the carriers is expected to be lower in the excited subbands than that in the first subband since the carriers in the former have a much larger effective mass.¹² According to the Shubnikov-de Haas data given in Table II, most of the carriers (more than 95% of total carriers) are residing in the first subband in samples with 60% and 65% In channels. The difference in energy between E_0 and E_1 also significantly increases in samples B and C. Therefore, it is not difficult to expect reduced intersubband scattering with increase of In mole fraction in the channel material. In conclusion, the increase in carrier confinement in the lowest subband and effects associated with it plays the most important role in the enhancement of low-field mobilities which is experimentally observed in the strained channel heterostructures. Alloy scattering limited mobility is also increased, by a factor of 10%, by the increase of the In content, when the $x(1-x)$ dependence is considered in the formula of the alloy scattering limited mobility.

B. High-field transport

Figure 3 shows the mobility-field characteristics obtained from pulsed Hall measurements on the different samples at 300 and 77 K. At 300 K, the mobility in all the samples is almost constant for $E < 500 \text{V/cm}$ and decreases

TABLE II. Transport data obtained from Hall and Shubnikov-de Haas (SDH) measurements.

Sample(x)	Hall data at 4.2 K		m^*/m_0	N_0^a (10^{12}cm^{-2})	N_1^b (10^{12}cm^{-2})	$E_1 - E_0^c$ (meV)
	μ_H ($\text{cm}^2/\text{V s}$)	n_H (10^{12}cm^{-2})				
A(0.53)	67 900	1.46	0.046 ± 0.002	1.12	0.26	43.2
B(0.60)	95 000	1.65	0.046 ± 0.002	1.53	0.04^d	76.1
C(0.65)	134 000	1.65	0.046 ± 0.002	1.65	0.04^d	84.6

^a Lowest subband occupation at 4.2 K determined from SDH measurements.

^b Occupation in first excited subband at 4.2 K.

^c Energy separation between ground state and first excited state in the 2DEG.

^d These values are approximate.

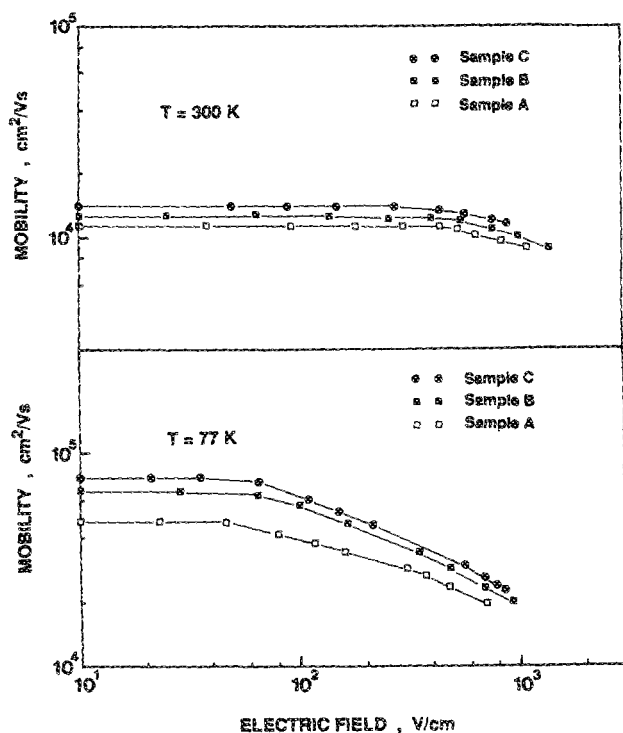


FIG. 3. 300- and 77-K mobility-field characteristics obtained from pulsed Hall measurements.

slightly at higher fields. All three samples show a similar trend in the measured electric-field range. It is clear that samples with excess In in the channel exhibit higher high-field mobilities in the entire electric-field range of measurement. The mobility of different temperatures and electric fields is limited by the different scattering mechanisms discussed in the previous section. At 300 K, electrons are predominantly scattered by polar-optical phonons at both the low and high electric-field ranges used in the pulsed Hall measurements. At 77 K, alloy scattering may be more dominant in the low electric-field regime. However, optical phonon scattering becomes dominant again as the electric field approaches 1 kV/cm. This may explain the observation that the difference in mobility between samples decreases as the electric field increases, as seen in the 77-K data. Intersubband scattering can also have a significant effect on the high-field characteristics since carriers have sufficient energy to be excited to the higher subband having higher effective masses in the electric-field range above 1 kV/cm.¹³

The velocity-field characteristics of electrons obtained from pulsed current-voltage measurements at room temperature are shown in Fig. 4. The electron velocity was calculated from the output current density recorded on a sampling oscilloscope. Measurements were made up to fields of 2.25 kV/cm and electron velocities were observed to increase monotonically in all three samples. Maximum velocities of 1.35 , 1.45 , and 1.55×10^7 cm/s were calculated at $E = 2.25$ kV/cm for samples A, B, and C, respectively. It is to be noted that no velocity saturation was observed at room temperature in any of the samples. The velocities of 77 K, shown in Fig. 4, were obtained from the measured mobility-

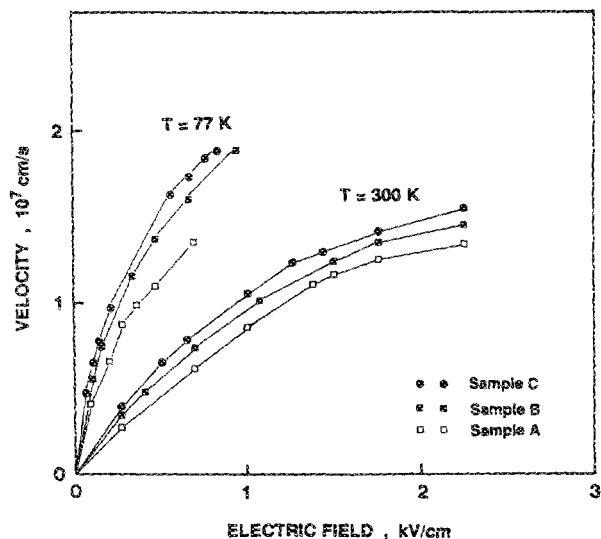


FIG. 4. Velocity-field characteristics obtained from pulsed current-voltage measurements and pulsed Hall measurements at 300 and 77 K, respectively.

field characteristics of Fig. 3 by using the relation

$$v(E) = \mu(E)E. \quad (1)$$

It is clear that electron velocities are increased with an increase in In content in the channel in the entire range of electric fields scanned during the measurements. It is also expected that velocity saturations will occur at higher fields, but these cannot be accurately measured due to the onset of instabilities.⁶ The enhancement of electron velocity is thought to be the main contributor to the superior device performance observed in samples B and C compared to that in sample A.

IV. CONCLUSIONS

A systematic study of the low- and high-field transport properties in MBE-grown pseudomorphic $\text{In}_x\text{Ga}_{1-x}\text{As}/\text{In}_{0.52}\text{Al}_{0.48}\text{As}$ heterostructure has been made. The Hall mobilities measured in these structures are extremely high and values of 13 900, 74 000, and 134 000 $\text{cm}^2/\text{V s}$ at 300, 77, and 4.2 K, respectively, have been measured in a sample with $x = 0.65$. We believe that this improvement results from a combination of reduced intersubband scattering, reduced impurity scattering (due to larger sheet charges), and reduced alloy scattering. The mobilities remain consistently high at high electric field up to 1 kV/cm. The high-field carrier velocities were independently measured in the same samples by pulsed current-voltage and pulsed Hall measurements. Once again, the velocities increase monotonically with field and with increase of In content in the channel region. In conclusion, we believe that the improvement in the performance of this class of devices results principally from the larger conduction band offset and the higher 2DEG velocities.

ACKNOWLEDGMENTS

We gratefully acknowledge the help provided by R. Reifenger and D. Miller of Purdue University during the

Shubnikov-de Haas measurements. We also thank Professor J. Singh and Professor S. Datta for several stimulating discussions. The work is being supported by the Army Research Office (URI Program) under Contract No. DAAL03-87-K-0007 and Wright Patterson Air Force Base under Contract No. F33615-87-C-1406.

¹M. Jaffe, Y. Sekiguchi, J. Singh, Y. Chen, D. Pavlidis, and M. Quillec, presented at the 1987 IEEE/Cornell Conference on Advanced Concepts in High Speed Semiconductor Devices and Circuit, Cornell University, Ithaca, NY, August 10-12 1987.

²C. Peng, S. Sinha, and H. Morkoç, *J. Appl. Phys.* **62**, 2880 (1987).

³H. Griem, K. Hsieh, I. D'Haenens, M. Delaney, J. Henige, G. Wicks, and A. Brown, Proceedings of the 7th MBE Workshop, Massachusetts Insti-

tute of Technology, Cambridge, MA, edited by D. L. Miller (AIP, New York, 1987), pp. 785-791.

⁴J. Kuo, B. Lalevic, and T. Chang, *IEEE IEDM Tech. Dig.*, 460 (1986).

⁵Y. Chan, D. Pavlidis, G. Ng, M. Jaffe, J. Singh, and M. Quillec, *IEEE IEDM Tech. Dig.*, 427 (1987).

⁶W. Hong and P. Bhattacharya, *IEEE Trans. Electron Devices ED-34*, 1491 (1987).

⁷P. Basu and B. Nag, *Appl. Phys. Lett.* **43**, 689 (1983).

⁸G. Bastard, *Appl. Phys. Lett.* **43**, 591 (1983).

⁹J. Lee and M. Vasselli, *Jpn. J. Appl. Phys.* **23**, 1086 (1984).

¹⁰V. Arora and A. Naeem, *Phys. Rev. B* **31**, 3887 (1985).

¹¹A. Kastalsky, R. Dingle, K. Chang, and A. Cho, *Appl. Phys. Lett.* **41**, 274 (1982).

¹²S. Mori and T. Audo, *J. Phys. Soc. Jpn.* **48**, 865 (1980).

¹³K. Tsubaki, A. Livingstone, M. Kawashima, H. Okamoto, and K. Kumabe, *Solid State Commun.* **46**, 517 (1983).